

Electronic Supplementary Information

An Unexpected Non-conjugated AIEgen with Discrete Dimer for Pure Intermolecular Through-Space Charge Transfer Emission

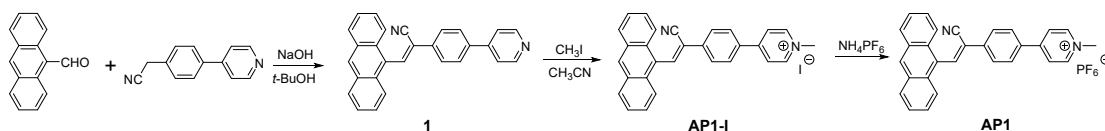
Xiujie Jiang,^{a#} Wei Tao,^{a#} Cheng Chen,^a Guoyong Xu,^a Haoke Zhang^{bc*} and Peifa Wei^{ac*}

a. Institutes of Physical Science and Information Technology, Key Laboratory of Structure and Functional Regulation of Hybrid Materials of Ministry of Education, Anhui University, Hefei, China.

b. MOE Key Laboratory of Macromolecular Synthesis and Functionalization, Department of Polymer Science and Engineering, Zhejiang University, Hangzhou, China ZJU-Hangzhou Global Scientific and Technological Innovation Center, Hangzhou 311215, China.

c. Guangdong Provincial Key Laboratory of Luminescence from Molecular Aggregates, South China University of Technology, Guangzhou, China.

All reagents were commercially available and used as supplied without further purification. Solvents were either employed as purchased or dried according to procedures described in the literature. NMR spectra were recorded on a Bruker Advance DMX 400 MHz spectrophotometer with deuterated solvent as the lock and residual solvent or tetramethylsilane (TMS) as the internal reference. Chemical shifts were reported relative to residual solvent signals. High-resolution mass spectra were obtained on a Finnigan MAT TSQ 7000 Mass Spectrometer operated at MALDI-TOF mode or a Bruker Daltonics Apex IV spectrometer at ESI mode. Absorption and photoluminescence spectra were recorded on a UV-Vis Spectrophotometer U-3900 spectrophotometer and a spectrofluorometer FS 5, respectively. Fluorescent microscopy images were acquired at an excitation wavelength of 365 nm using a Nikon Ni-U Fluorescence Microscope equipped. The lifetime was measured on a Horiba Fluoro max plus equipped with a xenon arc lamp (Xe900). The absolute fluorescence quantum yields were recorded on a Fluormax-4P spectrometer. Thermogravimetric analysis (TGA) was carried out on a Shimadzu-50 thermo-analyser under flowing N₂ with a heating rate of 10 °C/min. The X-ray diffraction (XRD) patterns of all as-prepared samples were collected by a X-ray diffractometer (Japan Rigaku D/MAX- γ A) with Cu-K α radiation ($\lambda = 0.154$ nm). The crystal data were collected on a Stoe Stadivari instrument.



Scheme S1. Synthetic route of AP1.

9-Anthracenecarboxaldehyde (233.6 mg, 1.13 mmol) and 2-(4-(pyridin-4-yl) phenyl) acetonitrile (20 mg, 1.03 mmol) were dissolved in 40 mL of *t*-BuOH. NaOH (90.6 mg, 2.27 mmol) in 5 mL of *t*-BuOH was added dropwise into the previous solution. After stirring overnight at room temperature, yellow precipitates formed. The mixture was filtered and *t*-BuOH was removed on a rotary evaporator. The residue was washed with *t*-BuOH to afford **1** as yellow solid (330 mg, 83.7%). The ¹H NMR spectrum of **1** was shown in Figure S1. ¹H NMR (CDCl₃, 293 K, 400 MHz), δ (ppm): 8.73-8.75 (m, 2H), 8.54-8.56 (m, 2H), 8.05-8.10 (m, 4H), 8.01-8.03 (m, 2H), 7.81-7.84 (m, 2H), and 7.51-7.60 (m, 6H). The ¹³C NMR spectrum of **1** was shown in Figure S2. ¹³C NMR (CDCl₃, 293 K, 400 MHz), δ (ppm): 76.8, 77.1, 77.3, 77.4, 116.4, 120.6, 121.6, 125.0, 125.7, 126.9, 127.0, 127.6, 128.0, 129.3, 129.4, 129.5, 131.4, 134.0, 139.6, 140.9, 147.1, and 150.6. HRMS (Figure S3): m/z calcd for [M + H]⁺ C₂₈H₁₉N₂ 383.1470; found 383.1536.

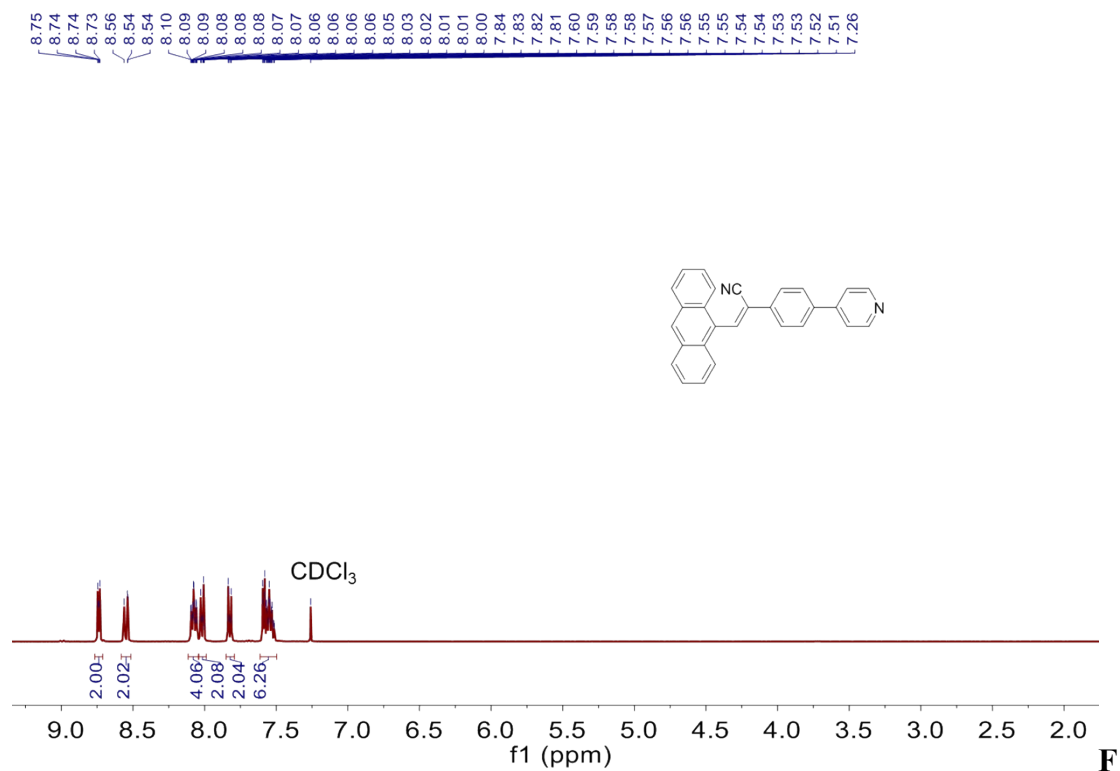


figure S1. $^1\text{H NMR}$ spectrum of **1** in CDCl_3 .

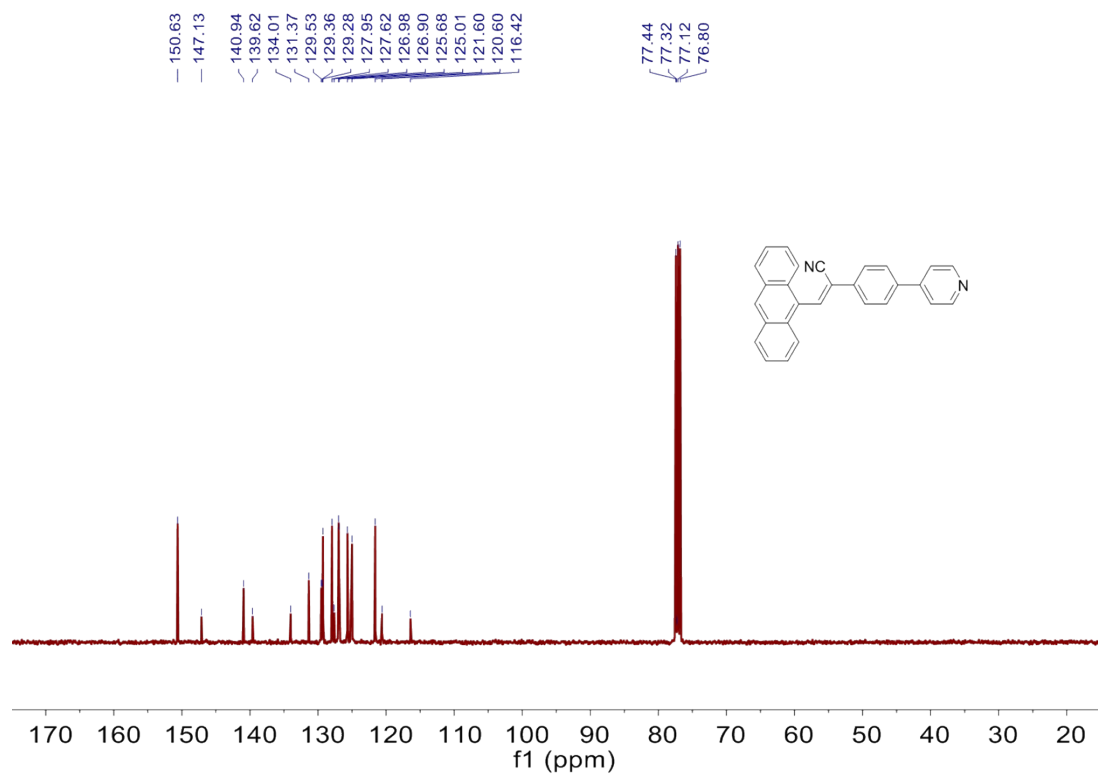


Figure S2. $^{13}\text{C NMR}$ spectrum of **1** in CDCl_3 .

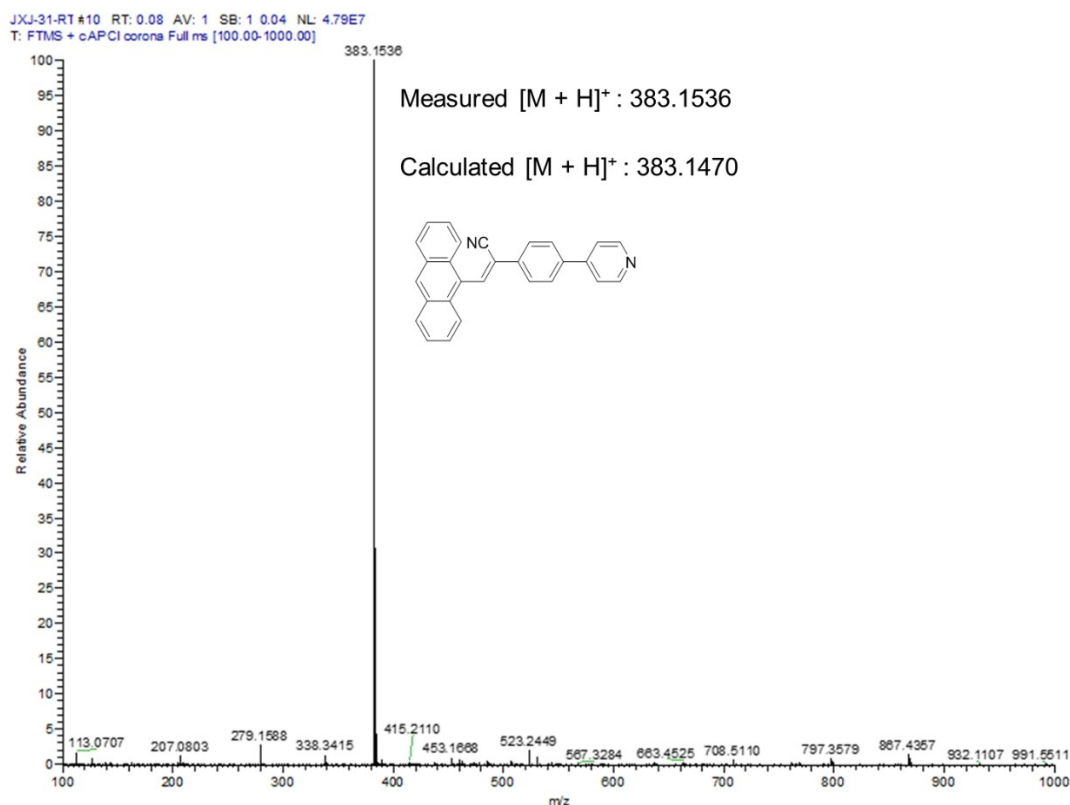


Figure S3. MALDI-TOF mass spectrum of **1**.

CH₃I (5.00 mL) was added into a solution of **1** (300 mg, 0.78 mmol) in CH₃CN. The mixture was heated to reflux. After 24 h, the reaction mixture was cooled to room temperature. The bright yellow precipitates formed were collected by suction filtration and washed with CH₃CN to afford **API-I** (390.0 mg, 95.6%) as a yellow solid. Then saturated aqueous NH₄PF₆ solution was added into the aqueous solution of **API-I**. The precipitates were collected by suction filtration and recrystallized from deionized water to afford **API** (360 mg, 91.6%) as an orange solid. The ¹H NMR spectrum of **API** was shown in Figure S4. ¹H NMR (CD₃CN, 293 K, 400 MHz), δ (ppm): 8.85 (s, 1H), 8.70 (s, 1H), 8.64-8.66 (t, 2H, *J* = 8 Hz), 8.30-8.32 (t, 2H, *J* = 8 Hz), 8.10-8.18 (m, 8H), 7.59-7.63 (m, 4H), and 4.31 (s, 3H). The ¹³C NMR spectrum of **API** was shown in Figure S5. ¹³C NMR (CD₃CN, 293 K, 400 MHz), δ (ppm): 47.7, 116.3, 117.4, 120.1, 125.0, 125.3, 125.9, 127.0, 127.5, 128.1, 129.0, 129.7, 129.2, 129.3, 131.3, 134.8, 136.8, 143.7, 145.4, and 155.0. HRMS (Figure S6): *m/z* calcd for $[M - PF_6]^+ C_{29}H_{23}N_2$ 397.1699; found 397.1690.

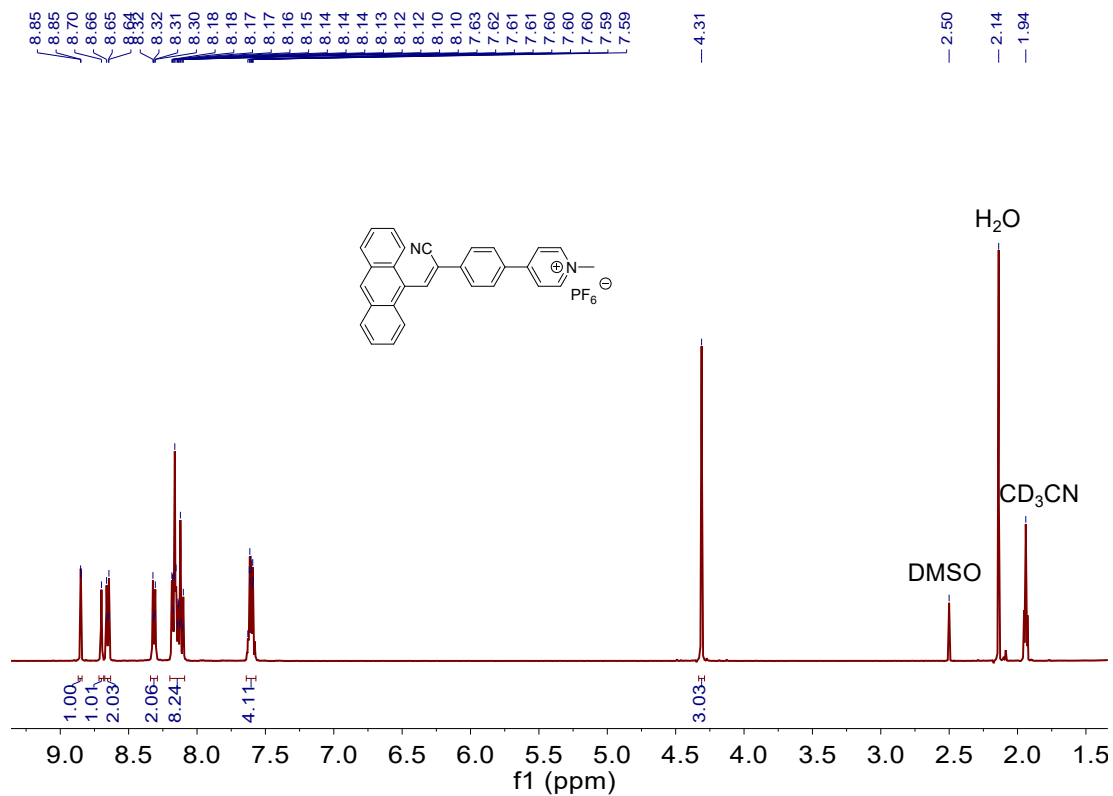


Figure S4. ¹H NMR spectrum of API in CD₃CN.

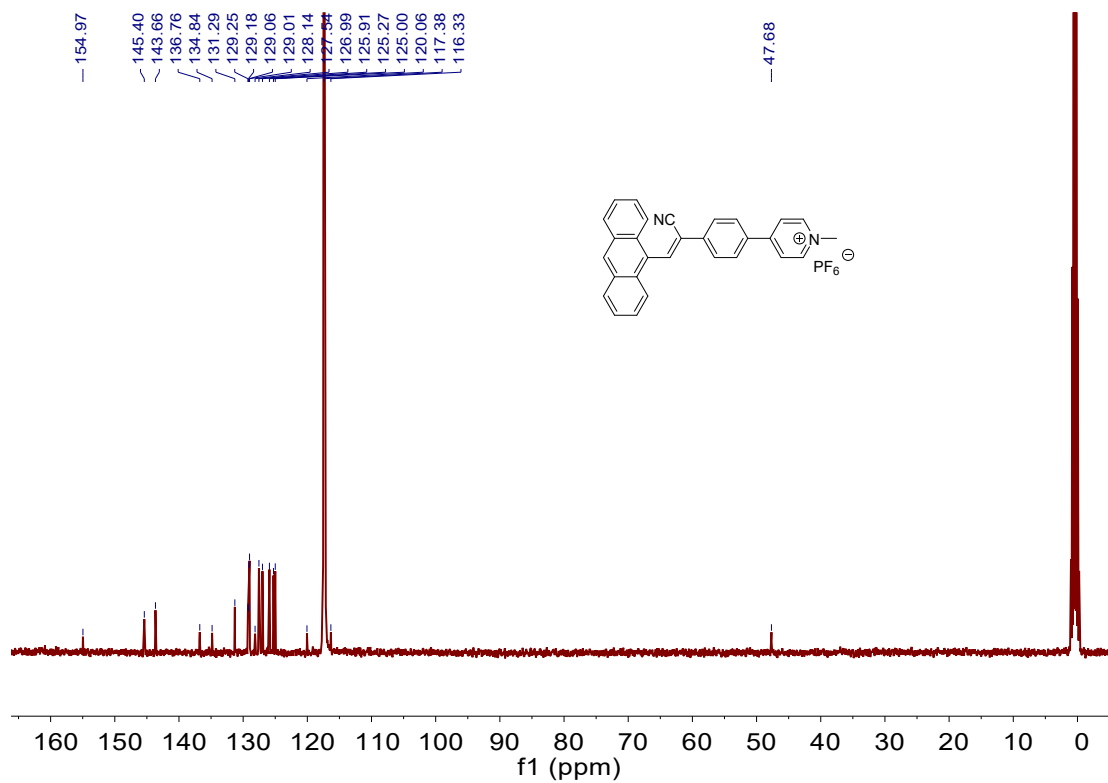


Figure S5. ¹³C NMR spectrum of API in CD₃CN.

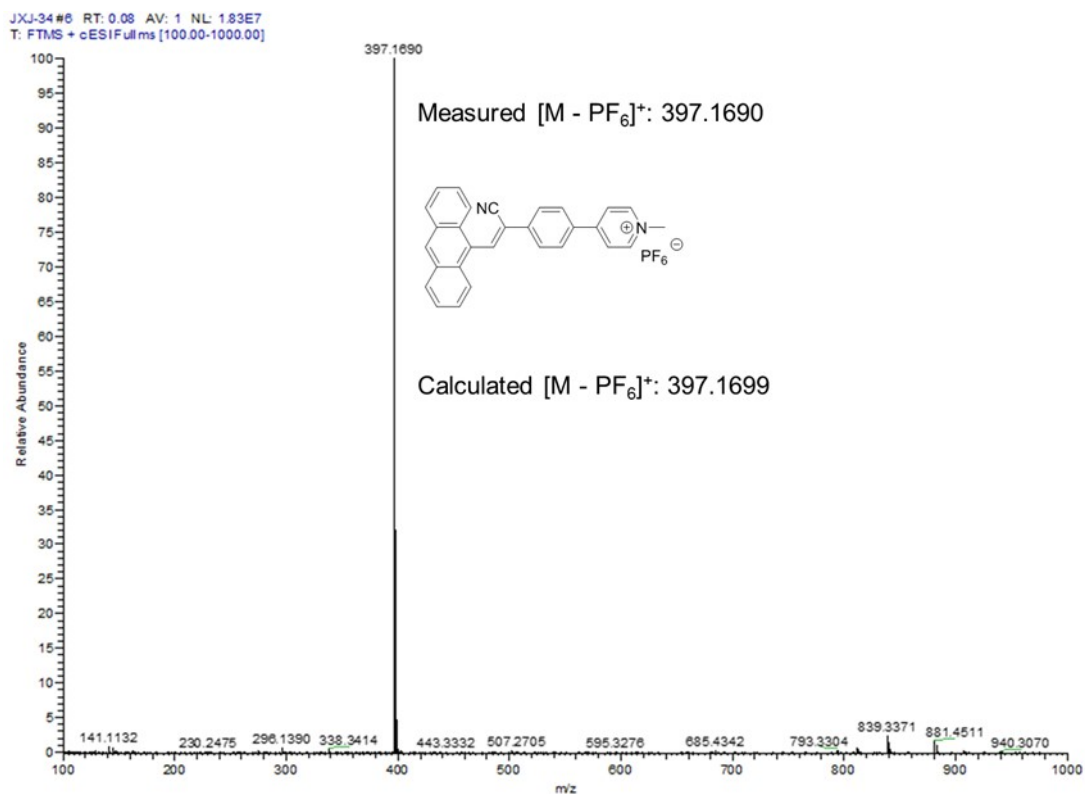
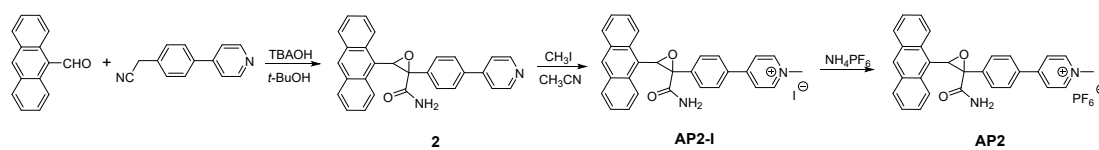


Figure S6. MALDI-TOF mass spectrum of AP1.



Scheme S2. Synthetic route of AP2.

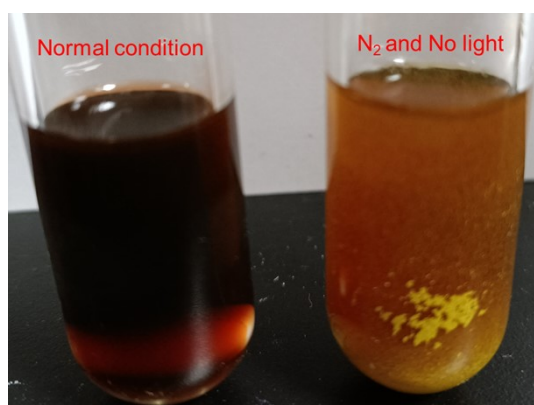
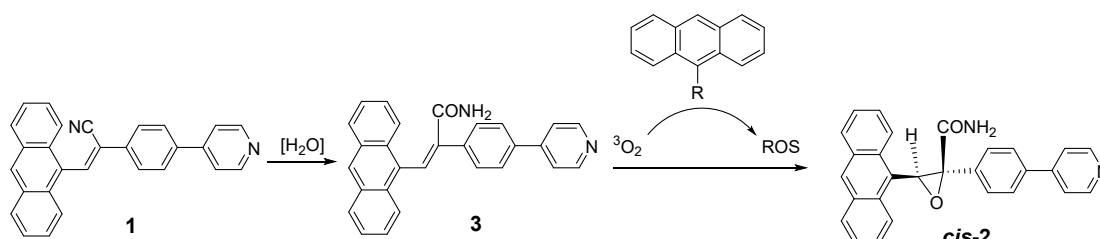


Figure S7. The picture after reaction (TBAOH as the base) under different conditions: (left) without degassing and in the presence of light; (right) degassing and in the

absence of light. The product formed in the right bottle was confirmed to be π -conjugated acrylonitrile derivative **1**, while the left one was proved to be carboxamide-functionalised oxirane derivative **2** (as shown in the following Scheme S3).



Scheme S3. Proposed plausible reaction mechanism for the formation of *cis-2*.

9-Anthracenecarboxaldehyde (300.0 mg, 1.45 mmol) and 2-(4-(pyridin-4-yl) phenyl) acetonitrile (256.9 mg, 1.32 mmol) were dissolved in 45 mL of *t*-BuOH. Tetrabutylammonium hydroxide 40 wt % solution in MeOH (1.9 g, 2.91 mmol) in 5 mL of *t*-BuOH was added dropwise into the previous solution. After stirring overnight at room temperature, and then taken to dryness on a rotary evaporator. Followed by flash column chromatography using petroleum ether/ethyl acetate (2:1, *v/v*) gave the light yellow powder **2** (480 mg, 87.4%). The ^1H NMR spectrum of **2** was shown in Figure S8. ^1H NMR (CDCl_3 , 293 K, 400 MHz), δ (ppm): 8.83-8.85 (d, 1H, $J = 8$ Hz), 8.71-8.72 (d, 2H, $J = 4$ Hz), 8.49 (s, 1H), 8.24-8.30 (m, 3H), 8.02-8.07 (m, 2H), 7.80-7.83 (m, 2H), 7.59-7.62 (m, 4H), 7.50-7.58 (m, 2H), 5.86-5.87 (d, 1H, $J = 4$ Hz), 5.08 (s, 1H), and 4.61-4.62 (d, 1H, $J = 4$ Hz). The ^{13}C NMR spectrum of **2** was shown in Figure S9. ^{13}C NMR (CDCl_3 , 293 K, 400 MHz), δ (ppm): 29.8, 63.5, 66.9, 76.8, 77.1, 77.3, 77.4, 121.8, 124.3, 124.9, 125.3, 125.8, 126.7, 127.4, 128.0, 128.5, 128.9, 129.4, 132.2, 138.7, 147.9, 150.4, and 168.9. HRMS (Figure S10): m/z calcd for $[\text{M} + \text{H}]^+$ $\text{C}_{28}\text{H}_{21}\text{N}_2\text{O}_2$ 417.1525; found 417.1470.

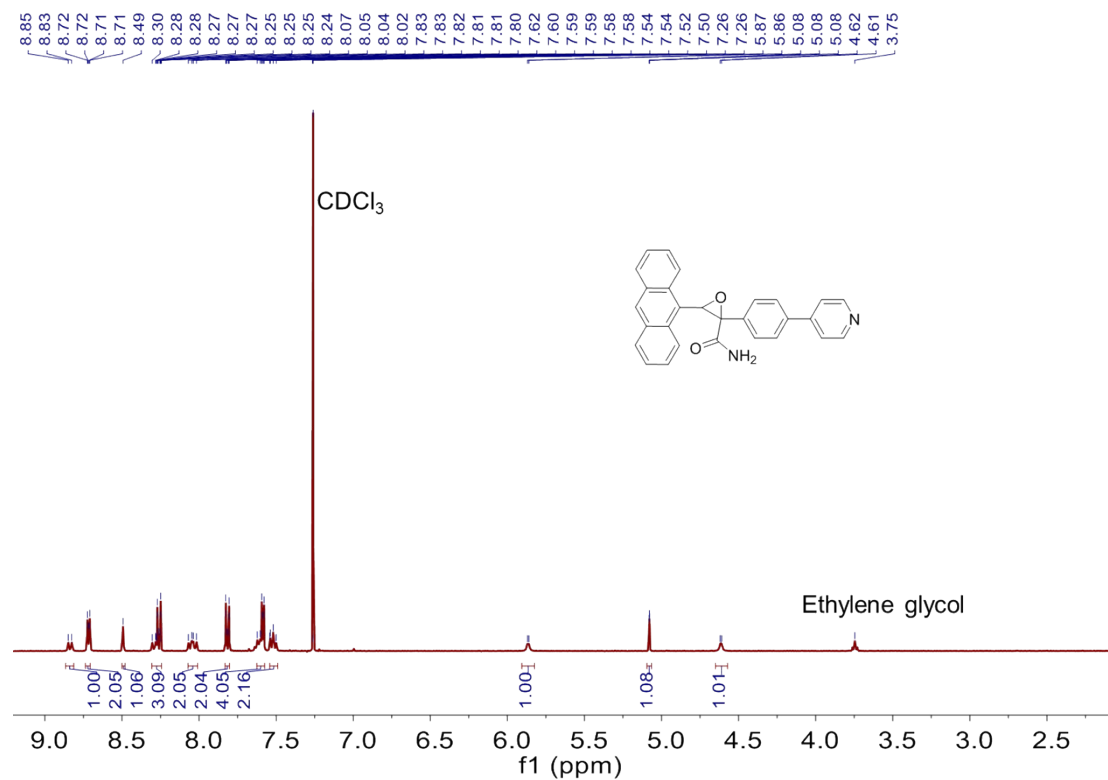


Figure S8. ^1H NMR spectrum of **2** in CDCl_3 .

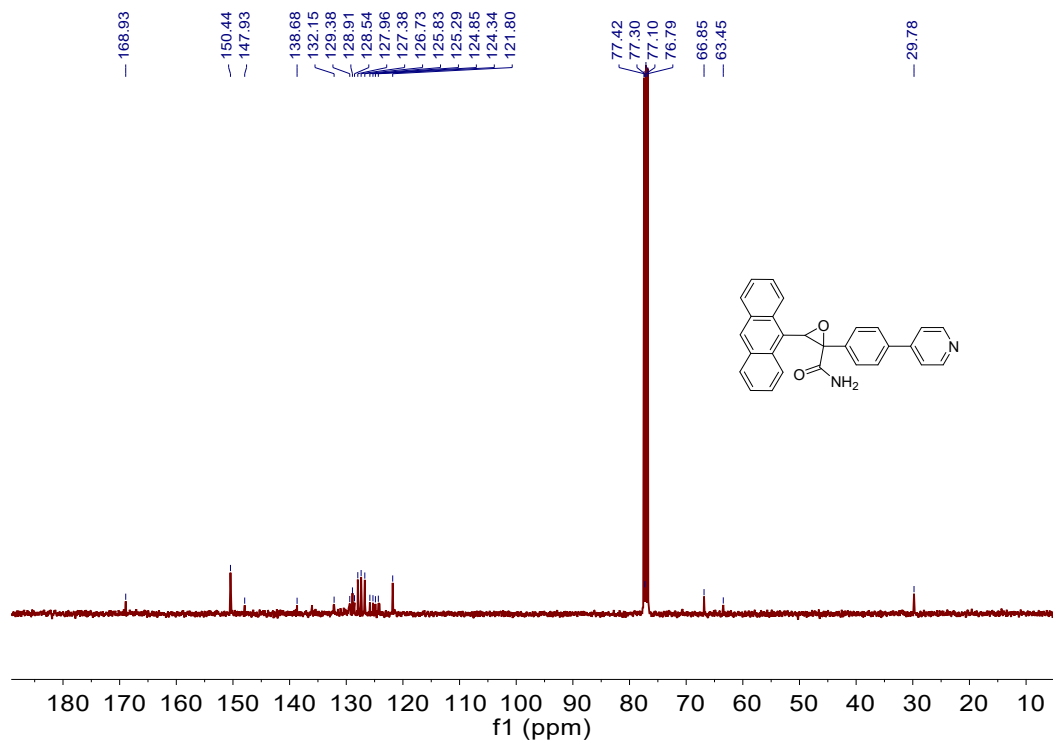


Figure S9. ^{13}C NMR spectrum of **2** in CDCl_3 .

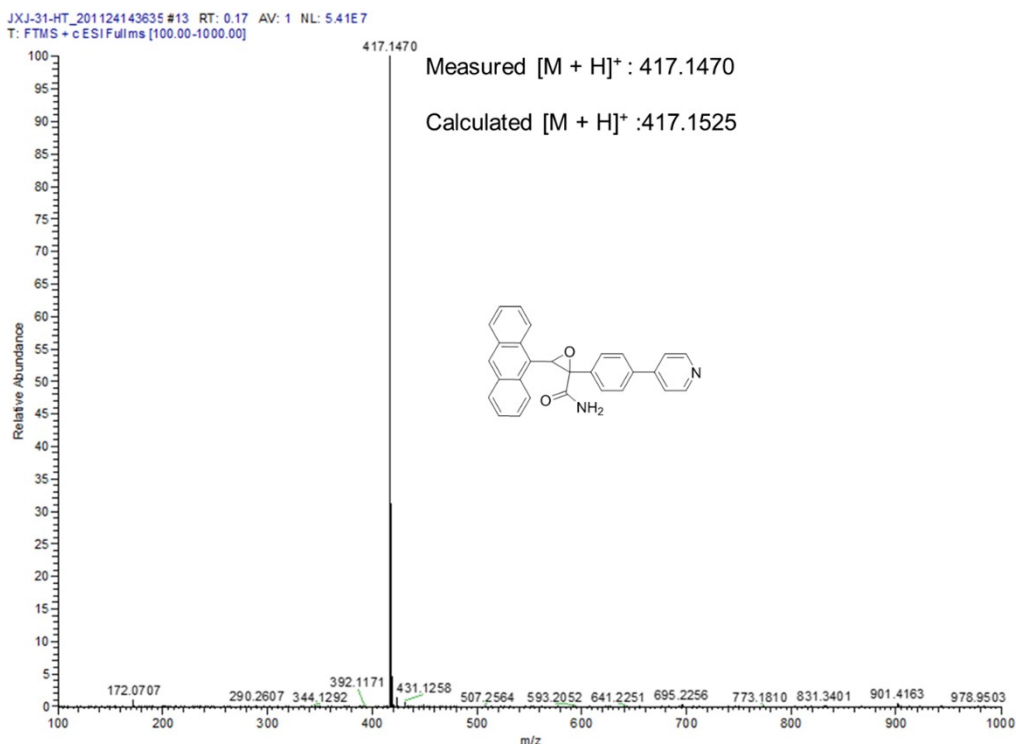


Figure S10. MALDI-TOF mass spectrum of **2**.

CH₃I (5.0 mL) was added into a solution of **2** (450.0 mg, 1.08 mmol) in CH₃CN. The mixture was heated to reflux. After 24 h, the reaction mixture was cooled to room temperature. The bright yellow precipitates formed were collected by suction filtration and washed with CH₃CN to afford **AP2-I** (535 mg, 88.9%) as a yellow solid. Then saturated aqueous NH₄PF₆ solution was added into the aqueous solution of **AP2-I**. The precipitates were collected by suction filtration and recrystallized from deionized water to afford **AP2** (480 mg, 87.1%) as a yellow solid. The ¹H NMR spectrum of **AP2** was shown in Figure S11. ¹H NMR (DMSO-*d*₆, 293 K, 400 MHz), δ (ppm): 9.05-9.07 (t, 2H, *J* = 8 Hz), 8.89-8.91 (d, 1H, *J* = 8 Hz), 8.66 (s, 1H), 8.57-8.59 (t, 2H, *J* = 8 Hz), 8.13-8.28 (m, 7H), 7.55-7.64 (m, 4H), 6.97 (s, 1H), 6.87 (s, 1H), 5.36 (s, 1H), and 4.36 (s, 3H). The ¹³C NMR spectrum of **AP2** was shown in Figure S12. ¹³C NMR (DMSO-*d*₆, 293 K, 400 MHz), δ (ppm): 39.4, 39.6, 39.9, 40.1, 40.3, 40.5, 40.7, 47.7, 63.5, 66.2, 124.8, 125.3, 125.8, 126.4, 126.8, 128.6, 128.6, 128.9, 129.1, 129.4, 130.4, 130.9, 131.6, 134.3, 140.3, 146.3, 154.3, and 168.2. HRMS (Figure S13): *m/z* calcd for $[M - PF_6]^+ C_{29}H_{23}N_2O_2$ 431.1754; found 431.1751.

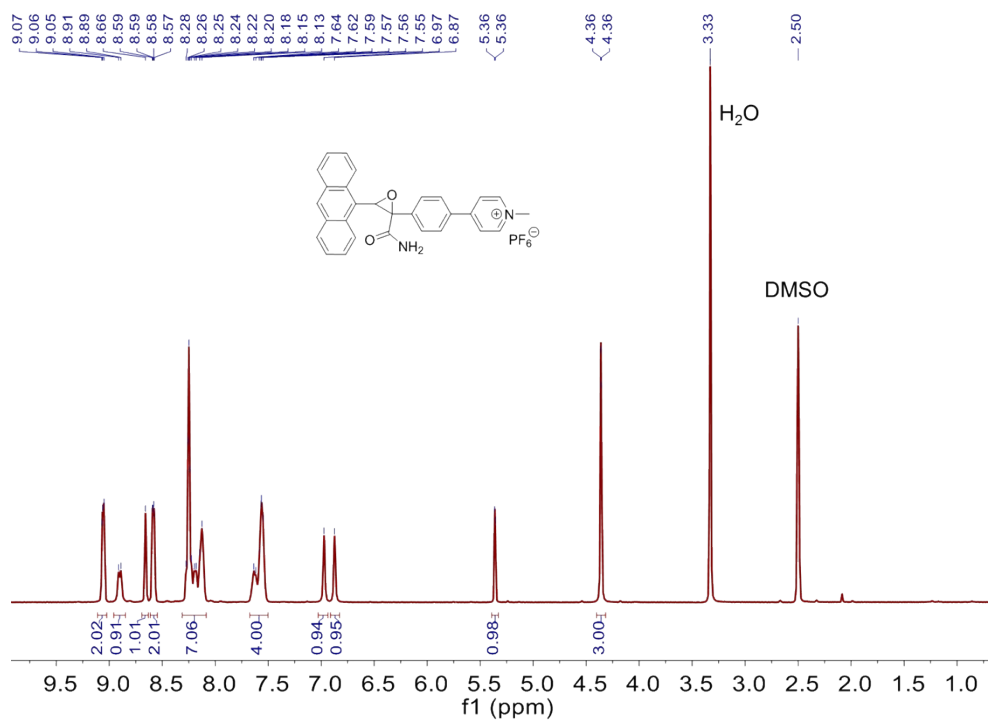


Figure S11. ^1H NMR spectrum of AP2 in $\text{DMSO-}d_6$.

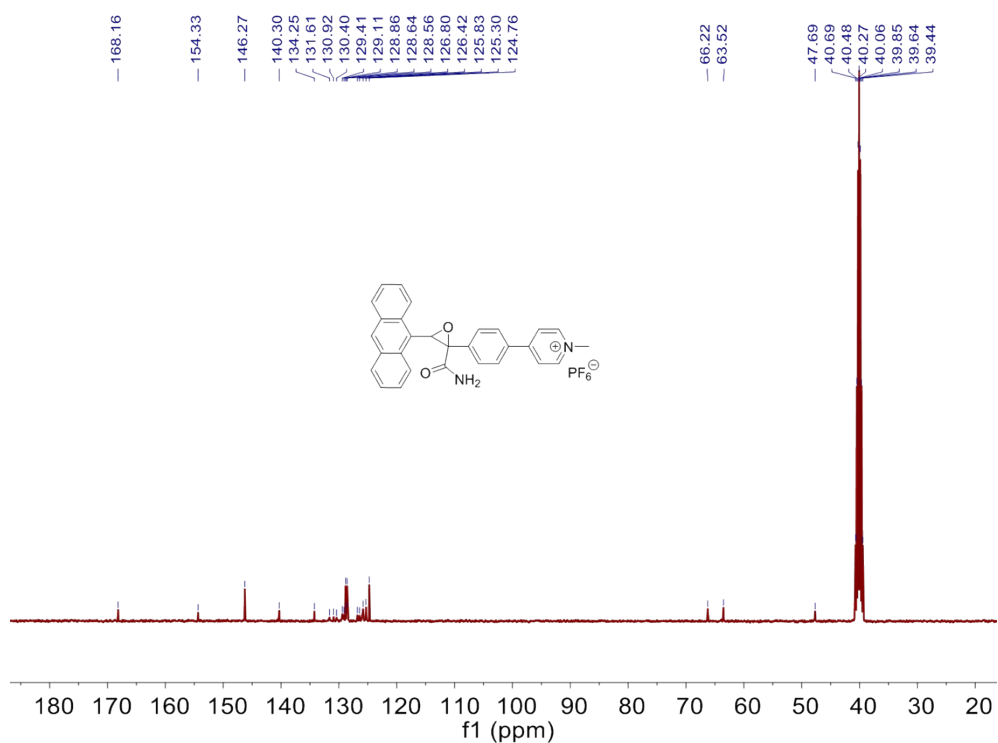


Figure S12. ^{13}C NMR spectrum of AP2 in $\text{DMSO-}d_6$.

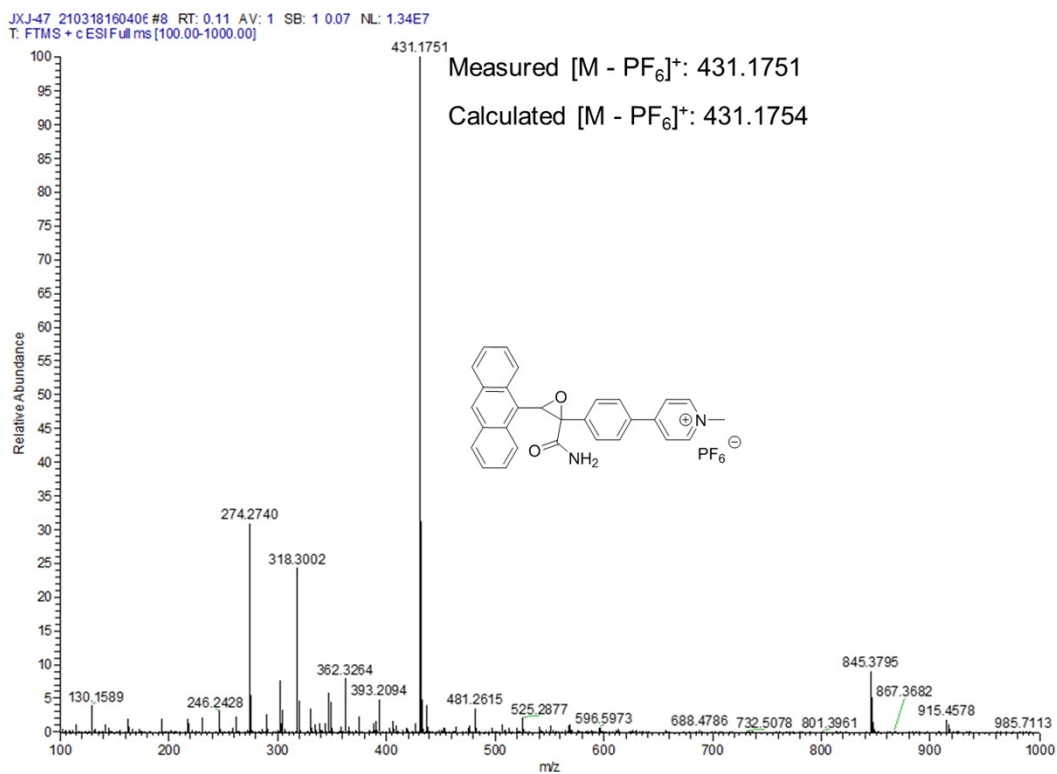


Figure S13. MALDI-TOF mass spectrum of AP2.

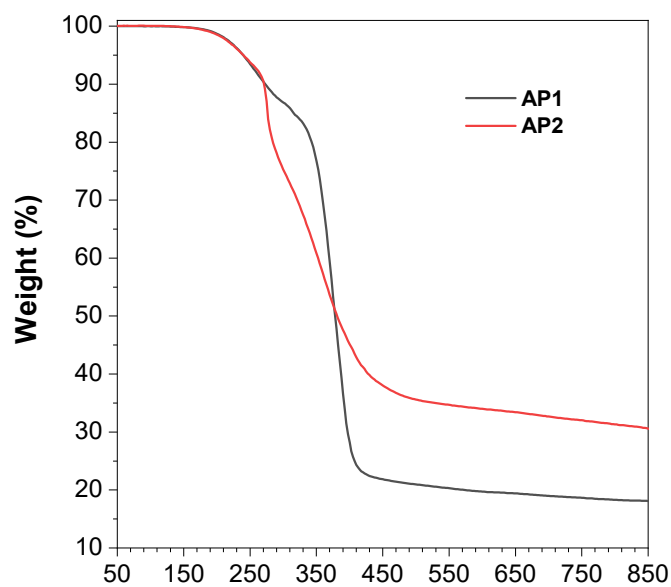


Figure S14. TGA thermogram of AP1 and AP2 recorded under nitrogen at a heating rate of 10 °C/min.

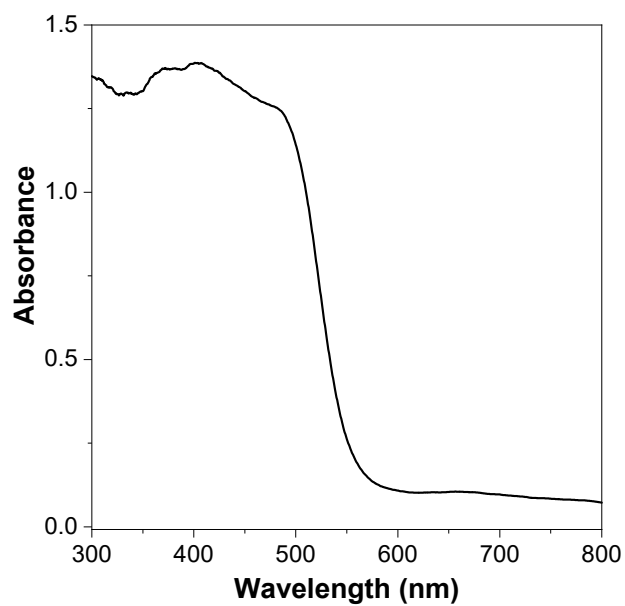


Figure S15. Absorption spectra of **AP1** in crystalline state.

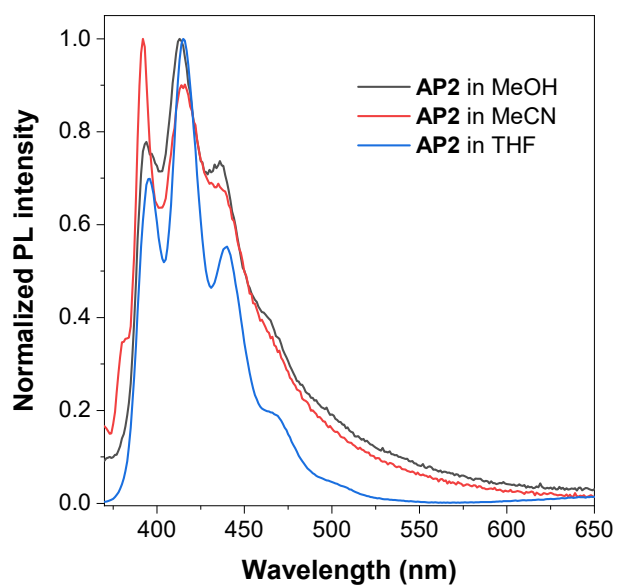


Figure S16. Normalized emission spectra of **AP2** in different solvents, $\lambda_{\text{ex}} = 350$ nm.

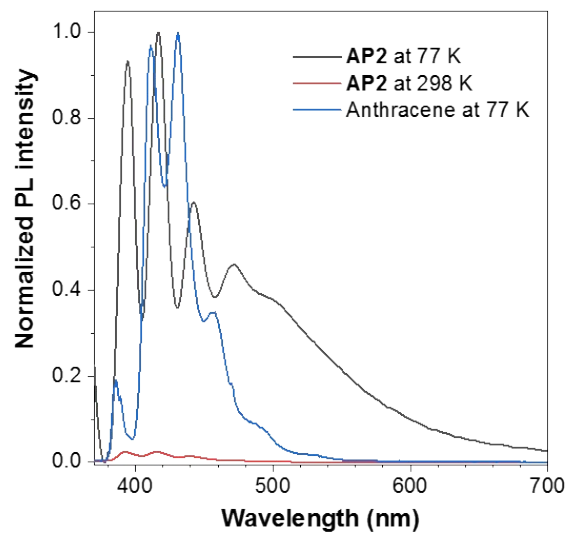
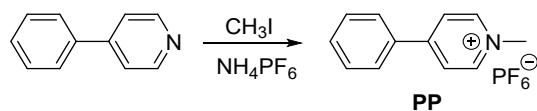


Figure S17. Normalized emission spectra of **AP2** and anthracene at 77 K and 298 K in THF, $\lambda_{\text{ex}} = 350$ nm. $c = 1.0 \times 10^{-6}$ mol/L.



Scheme S4. Synthetic route of **PP**.

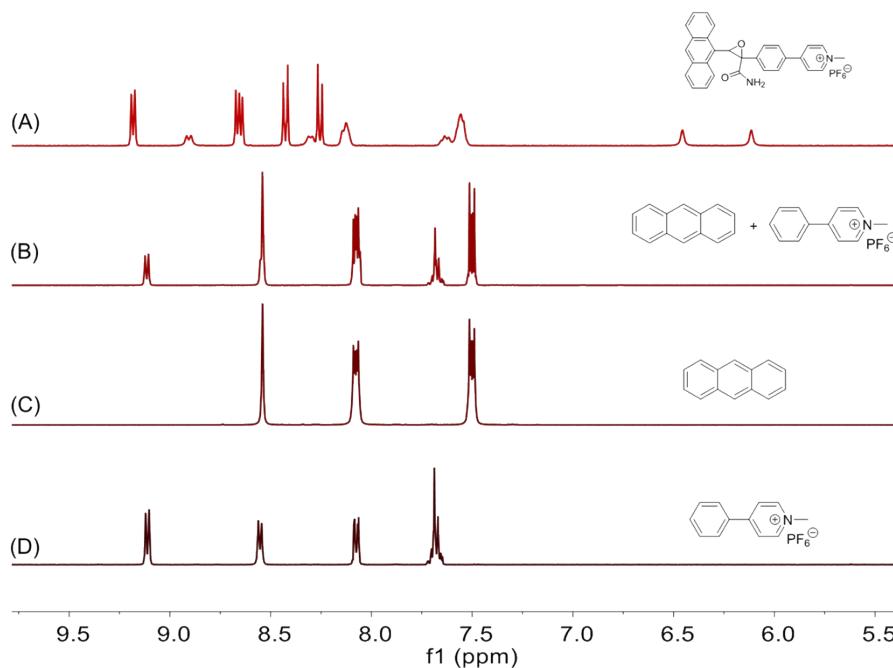


Figure S18. ^1H NMR spectra of (A) **AP2**. (B) **PP@An**. (C) anthracene and (D) **PP** in acetone- d_6 .

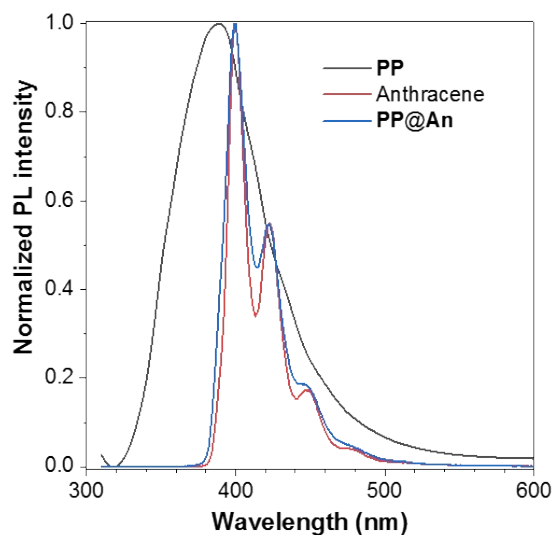


Figure S19. Normalized emission spectra of **PP**, anthracene, and **PP@An** in CH_3CN , $\lambda_{\text{ex}} = 290 \text{ nm}$.

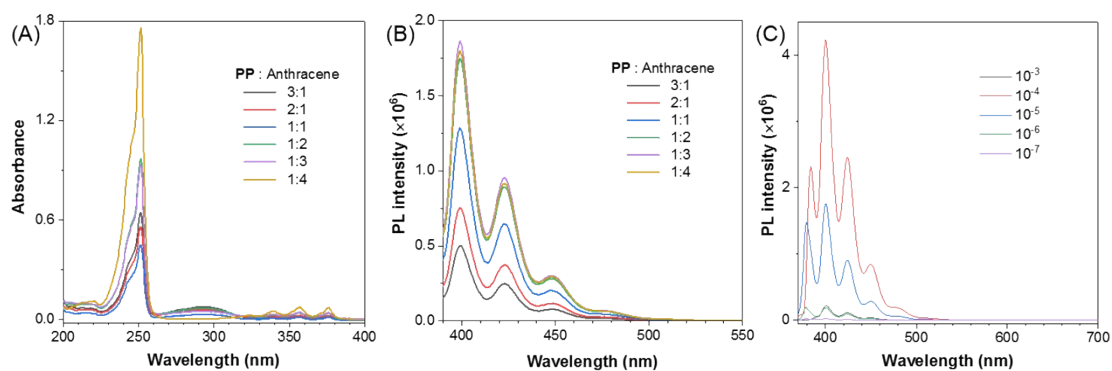


Figure S20. (A) Absorption spectra of **PP** and anthracene with different molar ratio in THF solution, $c = 10 \mu\text{M}$. (B) Emission spectra of **PP** and anthracene with different molar ratio in THF solution, $c = 10 \mu\text{M}$, $\lambda_{\text{ex}} = 350 \text{ nm}$. (C) Emission spectra of **PP@An** in THF solution with different concentration, $\lambda_{\text{ex}} = 350 \text{ nm}$.

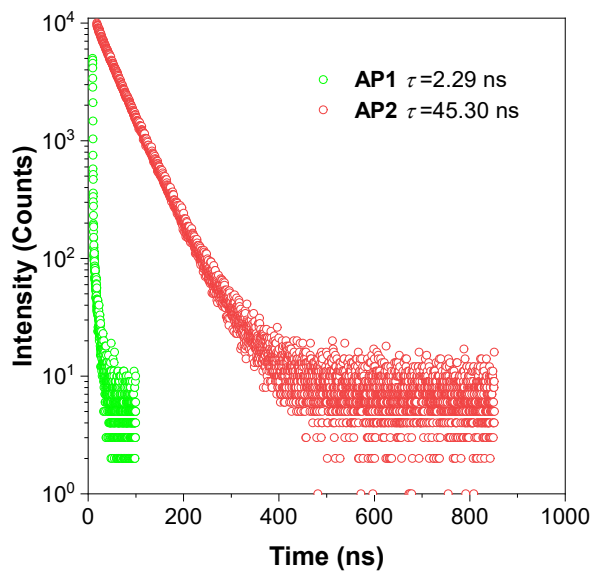


Figure S21. Time-resolved emission decays of AP1 and AP2 in crystal state.

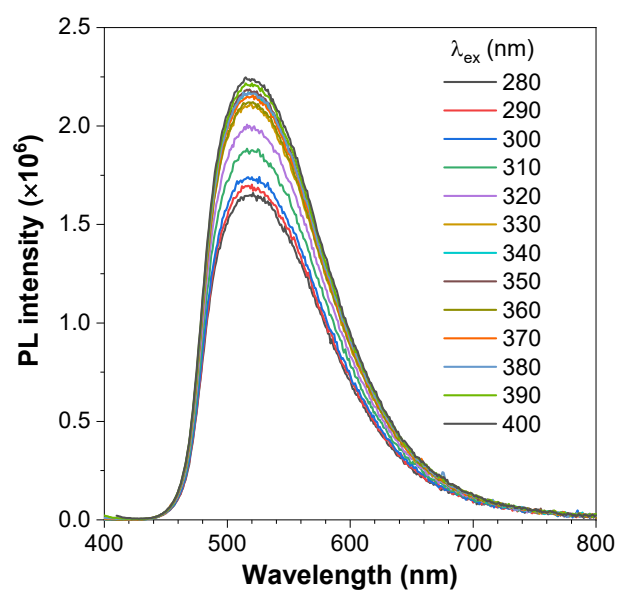


Figure S22. Emission spectra of AP2 crystal at different excitation wavelengths.

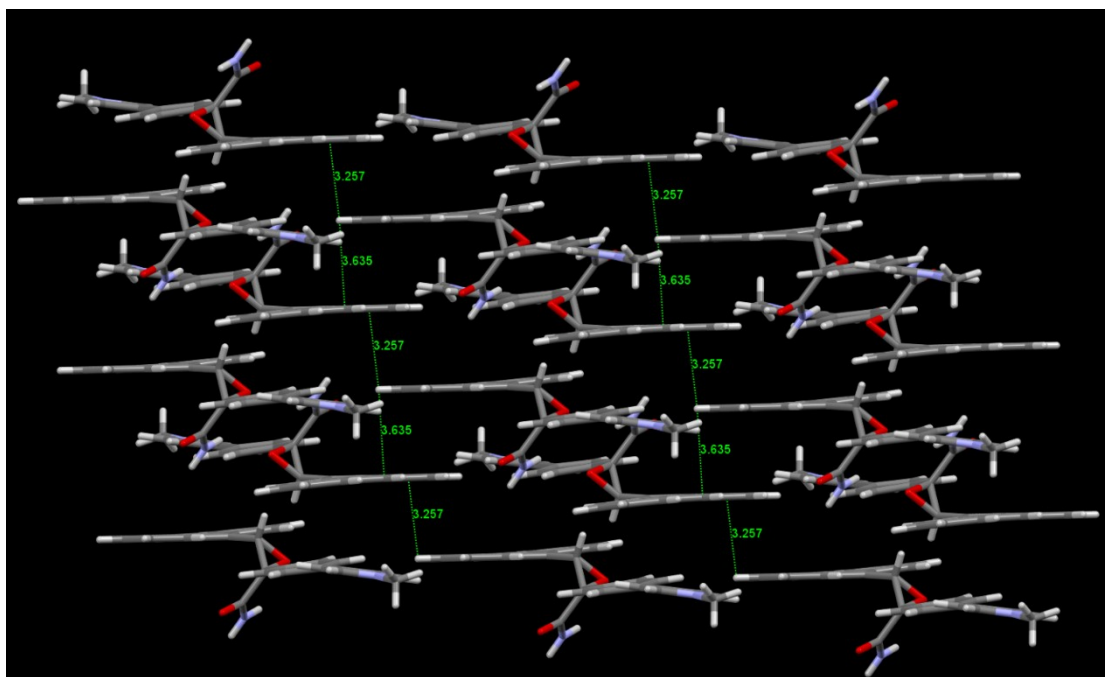
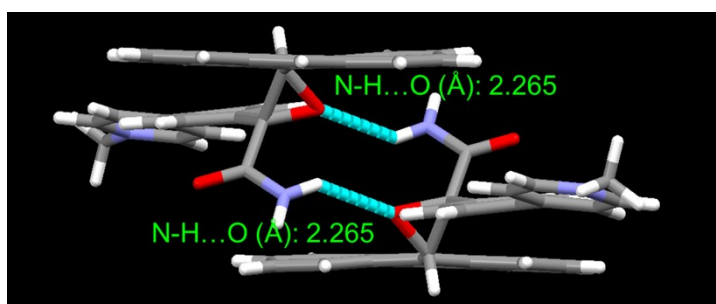
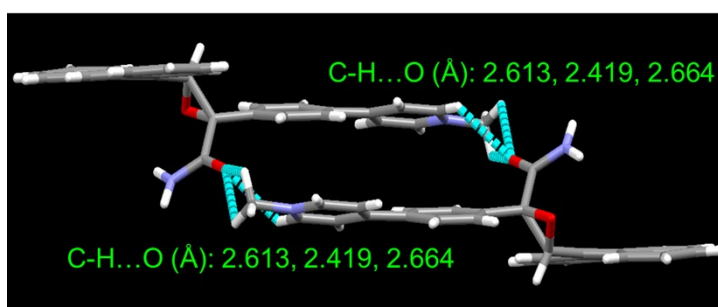


Figure S23. Crystal packing diagrams of AP2.



(Hydrogen bonds between the adjacent discrete dimer)



(Hydrogen bonds between the adjacent column)

Figure S24. The hydrogen bonds between the adjacent discrete dimers and columns in AP2

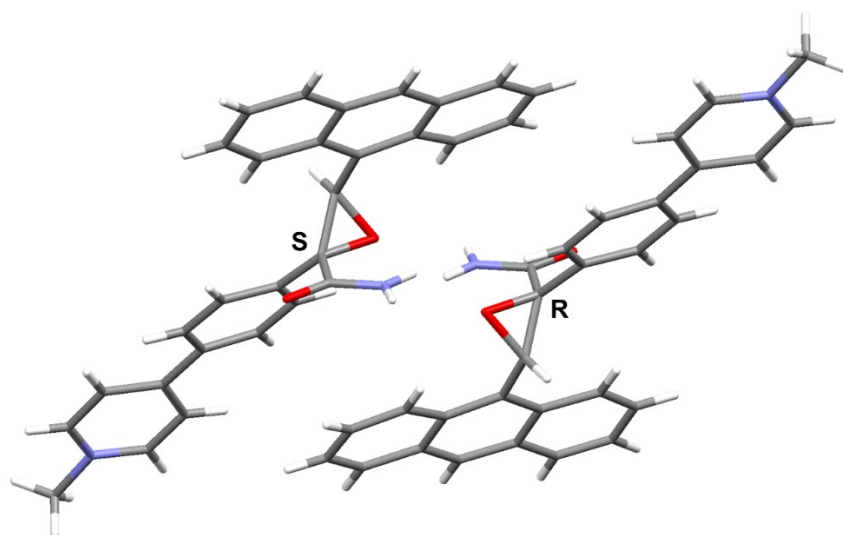


Figure 25. Stereo structure of one AP2 unit cell in the crystal.

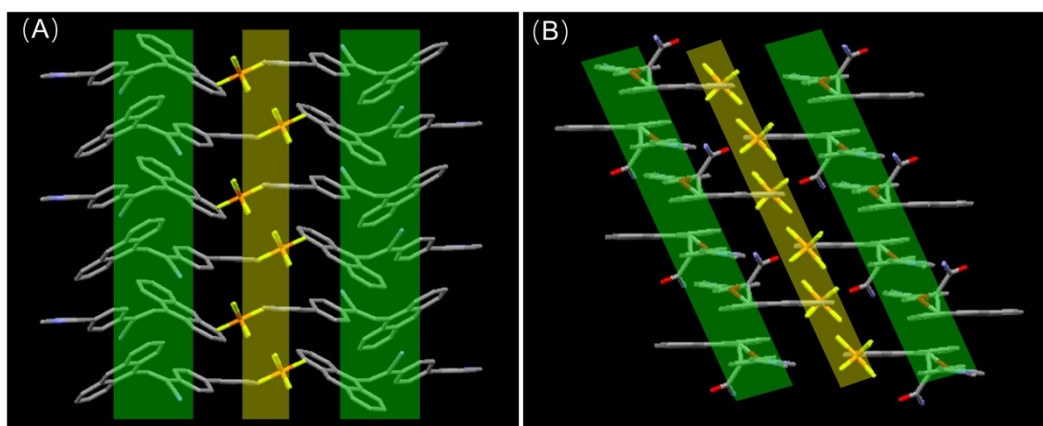


Figure 26. The illustration of the role of PF₆⁻ in (A) AP1 and (B) AP2 crystal packing.

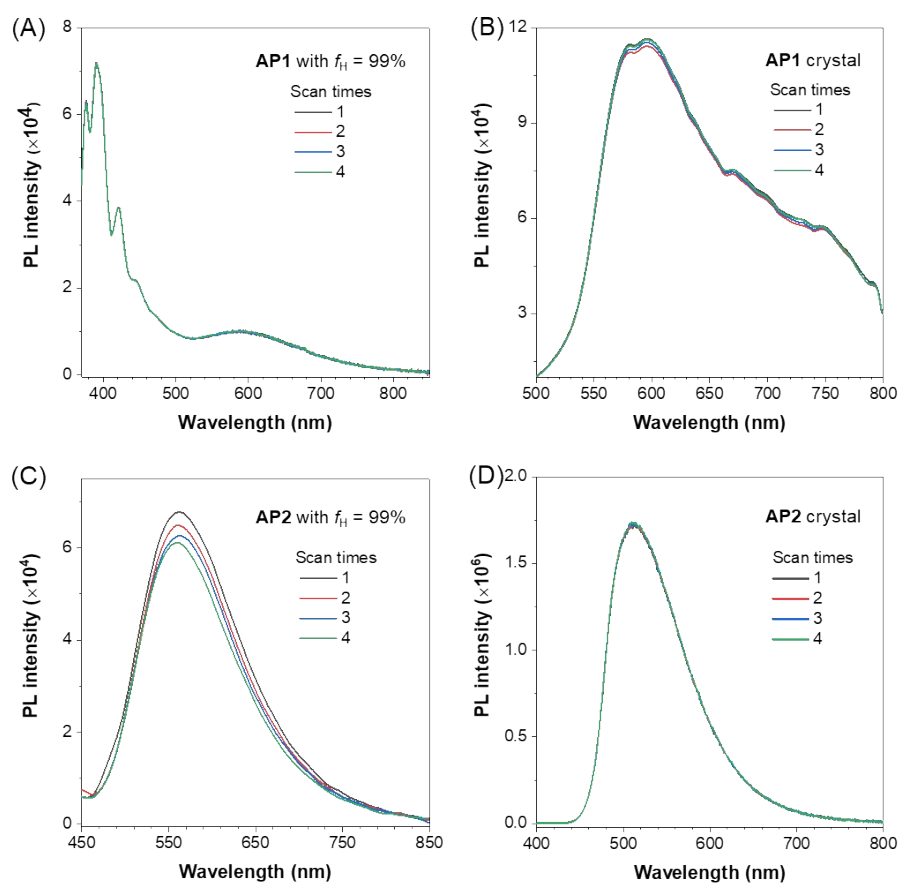


Figure S27. Emission spectra of AP1 (A and B) and AP2 (C and D) in aggregate state with $f_{\text{Hex}} = 99\%$ (A and C) and crystalline state (B and D) with different PL scan times.

Table S1. Crystal data and structure refinement for **AP1**.

Empirical formula	C ₂₉ H ₂₁ F ₆ N ₂ P
Formula weight	542.45
Temperature/ <i>K</i>	293 (2)
Crystal system	monoclinic
Space group	<i>P</i> 2 ₁ / <i>c</i>
<i>a</i> /Å	10.285
<i>b</i> /Å	8.039
<i>c</i> /Å	29.472
α /°	90
β /°	99.66
γ /°	90
Volume/Å ³	2402.2
<i>Z</i>	4
ρ_{calc} /cm ³	1.500
μ /mm ⁻¹	1.638
<i>F</i> (000)	1112.0
Crystal size/mm ³	0.3 × 0.2 × 0.1
Radiation	CuK α (λ = 1.54186)
2 Θ range for data collection/°	8.722 to 139.87
Index ranges	-10 ≤ <i>h</i> ≤ 12, -9 ≤ <i>k</i> ≤ 7, -24 ≤ <i>l</i> ≤ 35
Reflections collected	10428
Independent reflections	4356 [<i>R</i> _{int} = 0.0683, <i>R</i> _{sigma} = 0.0941]
Data/restraints/parameters	4356/0/344
Goodness-of-fit on <i>F</i> ²	1.012
Final <i>R</i> indexes [<i>I</i> >= 2 σ (<i>I</i>)]	<i>R</i> ₁ = 0.0605, <i>wR</i> ₂ = 0.1319
Final <i>R</i> indexes [all data]	<i>R</i> ₁ = 0.1218, <i>wR</i> ₂ = 0.1620
Largest diff. Peak/hole / e Å ⁻³	0.35/-0.33
CCDC	2090628

Table S2. Crystal data and structure refinement for **AP2**.

Empirical formula	C ₂₉ H ₂₃ F ₆ N ₂ O ₂ P
Formula weight	576.46
Temperature/ <i>K</i>	293 (2)
Crystal system	triclinic
Space group	<i>P</i> -1
<i>a</i> /Å	9.1654 (6)
<i>b</i> /Å	11.5906 (7)
<i>c</i> /Å	12.2355 (8)
α /°	96.138 (5)
β /°	97.787 (5)
γ /°	91.155 (5)
Volume/Å ³	1279.65 (14)
<i>Z</i>	2
ρ_{calc} /cm ³	1.496
μ /mm ⁻¹	1.632
<i>F</i> (000)	592.0
Crystal size/mm ³	0.3 × 0.2 × 0.1
Radiation	CuK α (λ = 1.54186)
2 Θ range for data collection/°	7.676 to 137.066
Index ranges	-11 ≤ <i>h</i> ≤ 9, -7 ≤ <i>k</i> ≤ 13, -14 ≤ <i>l</i> ≤ 14
Reflections collected	10292
Independent reflections	4539 [<i>R</i> _{int} = 0.0498, <i>R</i> _{sigma} = 0.0387]
Data/restraints/parameters	4539/120/417
Goodness-of-fit on <i>F</i> ²	1.037
Final <i>R</i> indexes [<i>I</i> >= 2 σ (<i>I</i>)]	<i>R</i> ₁ = 0.0786, <i>wR</i> ₂ = 0.2154
Final <i>R</i> indexes [all data]	<i>R</i> ₁ = 0.0880, <i>wR</i> ₂ = 0.2348
Largest diff. Peak/hole / e Å ⁻³	1.23/-0.95
CCDC	2090629